Improving the Quality of Photoacoustic Images using the Short-Lag Spatial Coherence Imaging Technique

Behanz Pourebrahimi, Sangpil Yoon, Dustin Dopsa, Michael C. Kolios
Department of Physics, Ryerson University, Toronto, Canada
mkolios@ryerson.ca

ABSTRACT

Clutter noise is an important challenge in photocoustic (PA) and ultrasound (US) imaging as they degrade the image quality. In this paper, the short-lag spatial coherence (SLSC) imaging technique is used to reduce clutter and side lobes in PA images. In this technique, images are obtained through the spatial coherence of PA signals at small spatial distances across the transducer aperture. The performance of this technique in improving image quality and detecting point targets is compared with a conventional delay-and-sum (DAS) beamforming technique. A superior contrast, contrast-to-noise ratio (CNR) and signal-to-noise ratio (SNR) are observed when SLSC imaging is employed. Point spread function of point targets shows an improved spatial resolution and reduced side lobes when compared with DAS beamforming. Also shown is the impact of increasing the number of frames on which SLSC is applied. The results show that contrast, CNR, and SNR are improved with increasing number of frames.

Keywords: photoacoustic, beamforming, short-lag spatial coherence, delay-and-sum, clutter, image quality.

1. INTRODUCTION

Medical imaging has played a key role in diagnostics and therapy. One of the challenges in medical imaging techniques is related to noise artifacts. Artifacts are misrepresentations of tissue structure caused by different phenomena such as data acquisition errors and imperfect reconstruction algorithms. Among different reconstruction algorithms, a recent technique for non-invasive imaging is PA imaging which is developed based on the PA effect. The PA effect refers to the generation of acoustic waves from an object being illuminated by pulsed or modulated electromagnetic radiation. PA imaging provides both the absorption contrast of light and the ultrasound imaging resolution. Just as in US imaging, PA imaging exhibits clutter artifacts.

In the literature, different techniques have been developed for PA imaging. The techniques used for ultrasound imaging can also be used for PA imaging as both techniques measure acoustic waves [1], [2]. Ultrasound imaging aims at reconstructing the reflectivity of a medium created by impedance mismatch between two regions. In comparison, PA imaging uses ultrasound signals generated by the thermal expansion of a region and depends on optical absorption and electromagnetic radiation. For ultrasound linear array detectors, the delay-and-sum (DAS) approach is the most popular beamforming technique in PA and ultrasound imaging. In DAS beamforming, an image is built based on the magnitude of the PA or ultrasound signals, generated through absorbed light or by backscattering, respectively. The basic concept of DAS beamforming is to sum the signals emitted from a point target after applying individual delays to each signal. Another approach developed in ultrasound imaging utilizes the spatial coherence of backscattered signals. The concept of accounting for spatial coherence from incoherent sources such as scatterers originated from optics [3]. This concept was adapted from optics and was used in the ultrasound field as a complimentary approach to suppress signals from off-axis targets and compensate phase aberration in reconstructed ultrasound images [4], [5], [6]. Spatial coherence in the short-lag region, referred to as short-lag spatial coherence (SLSC), has been applied to various clinical applications in ultrasound imaging [7] [8].

In this paper, the SLSC imaging technique is implemented for PA imaging. The performance of SLSC is compared with the DAS beamforming based on contrast, contrast-to-noise ratio (CNR), signal-to-noise ratio (SNR), as well as spatial resolution using reconstructed images of tissue mimicking phantoms.

2. MATERIALS AND METHODS

In the following sections, the experimental setup is firstly described and then the imaging technique is explained.

2.1. Phantoms

Two tissue mimicking phantoms, one with three point targets and another with an inclusion were used to study the SLSC technique in PA imaging. The phantoms are shown in Figure 1. The first phantom was used to explore the spatial resolution of t reconstructed PA images. Graphite rods with the diameter of 500 μm were used as point targets and placed in a background phantom. The phantom was made of 6-wt % gelatin (Type A, Sigma-Aldrich, Inc.) and 0.1-wt % titanium oxide (Sigma-Aldrich, Inc.). Three point targets were located at 4 mm, 9 mm, and 14 mm away from the surface of a linear array transducer during point target experiments. The second phantom was made to investigate contrast of PA images. The background portion of the phantom was constructed by following the same protocol as for the first phantom. The inclusion has a diameter of 4 mm in diameter and was made with 12-wt % gelatin, 0.1 wt % titanium oxide, and 0.05 wt % graphite (Sigma-Aldrich, Inc.). The inclusion was placed 12 mm away from the surface of the linear array transducer during inclusion experiments.

2.2. Photoacoustic Imaging System

The imaging system is composed of a pulsed laser, cuvette, Sonic RP imaging system (Ultrasonix Medical Corporation, Vancouver, Canada) with DAQ (Ultrasonix Medical Corporation, Vancouver, Canada), and a linear array transducer (L14-5/38, Prosonic Corporation, 7.2 MHz center frequency, 128 elements with 0.3048 mm element spacing, and 70 % fractional bandwidth). An optical parametric oscillating (OPO) laser (Vibrant II, Opotek, Inc.) produced 6 ns pulses with a 10 Hz pulse repetition rate at 760 nm wavelength. The fluence was 30 mJ/cm^2.

During the PA imaging experiments, phantoms were placed in a cuvette with two optical windows. Laser pulses passed through the optical window located at the bottom of the cuvette for point target experiments and at the front of the cuvette for inclusion experiments (Figure 1). The linear array transducer was placed slightly above the phantom to receive PA signals generated by both point targets and inclusion. A Sonic RP imaging system was interfaced with the linear array transducer to acquire radiofrequency (RF) data for off-line beamforming to reconstruct PA images. The DAS and SLSC techniques were used to generate images from the RF data collected from the experiments involving the point targets and the inclusion.
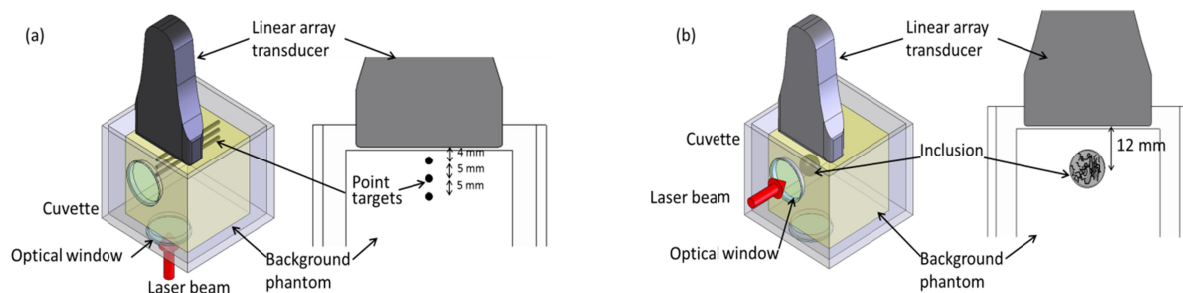

Figure 1. Schematic diagram of experimental setup. (a) A phantom with three point targets and (b) a phantom with an inclusion were placed inside a cuvette. Linear array transducer was placed at the top of the cuvette to receive photoacoustic signals generated by point targets and the inclusion illuminated by laser pulses.

2.3. Short-Lag Spatial Coherence Imaging

The short-lag spatial coherence (SLSC) imaging technique is based on the Van Cittert-Zernike (VCZ) theorem [9]. This theorem states that the spatial coherence of a wave emitted from incoherent sources is the scaled Fourier transform of the source's intensity distribution. The VCZ theorem can thus predict the spatial covariance of the pressure field created by a random medium, which behaves as an incoherent source [3]. In SLSC imaging, an image is formed based on the spatial coherence of acoustic waves generated by absorbed light. Acoustic waves are received by a transducer array and time delays are applied to compensate for the time difference in received signals. The spatial coherence of the wave fronts is computed for a number of adjacent transducer elements within a specific time interval. Considering a transducer with a receiving aperture of N elements, spatial coherence of the signals is computed by normalizing the covariance of the time delayed signals across the receive aperture given by the following equation [10]:

$$R(m) = \frac{1}{N-m} \sum_{i=1}^{N-m} \frac{\sum_{n=n_1}^{n_2}(s_i(n)-\mu_{s_i})(s_{i+m}(n)-\mu_{s_{i+m}})}{\sqrt{\sum_{n=n_1}^{n_2}(s_i(n)-\mu_{s_i})^2 \sum_{n=n_1}^{n_2}(s_{i+m}(n)-\mu_{s_{i+m}})^2}} \qquad (1)$$

where $s_i(n)$ and $s_{i+m}(n)$ are the time delayed signals received by i^{th} and $(i+m)^{th}$ elements of the transducer at time or depth n, μ_{s_i} and $\mu_{s_{i+m}}$ are the mean signals, m is the distance, or lag, in the number of elements between two points. The correlation kernel size $n_2 - n_1$ is the distance at which the wave fronts are observed. Spatial coherence is calculated for the distance which is chosen to be one wavelength. Then, the value of each pixel at each location n is computed as the sum of the spatial coherences over the first M lags.

$$R_{slsc} = \sum_{m=0}^{M} R(m) \qquad (2)$$

In this paper, we considered $M \cong 30\% \times N$, where N is the aperture size.

3. RESULTS

SLSC and DAS beamforming were used to reconstruct the photoacoustic (PA) images of the two phantoms with the graphite rods and the inclusion. Figures 3 and 5 show the reconstructed images. Figures 3(a) and 5(a) show the images created by SLSC technique and Figures 3(b) and 5(b) represent images reconstructed by DAS beamforming. For DAS beamforming, images are obtained by adding the amplitudes of delayed received signals and then applying the Hilbert transform. SLSC images were obtained based on spatial coherence of the signals at each depth computed by equations 1 and 2. The lag was considered to be 28% of the aperture size ($M = 9, N = 32$) which gave a good performance. The correlation kernel size ($n_2 - n_1$) was considered to be one wavelength based on the central frequency of receiving transducer. In PA, there is no transmitted beam and the received signals are generated by optical absorbers which typically emit broadband waves that are detected at frequencies within the range of receiving transducer bandwidth.

The ultrasound waves received by the transducer are assumed to be generated at the location where optically absorbing objects (the inclusion or graphite) are situated. The signals received from other locations in the image are likely related to clutter and/or the transducer side lobes. Clutter is created due to interfering signals and side lobes are generated from acoustic beam emitted off axis and sound velocity heterogeneity. As shown in Figures 3 and 5, greater side lobe signal and more clutter are observed in DAS beamforming compared to SLSC. Clutter and side lobes typically have low spatial coherence; therefore they are reduced when SLSC is applied.
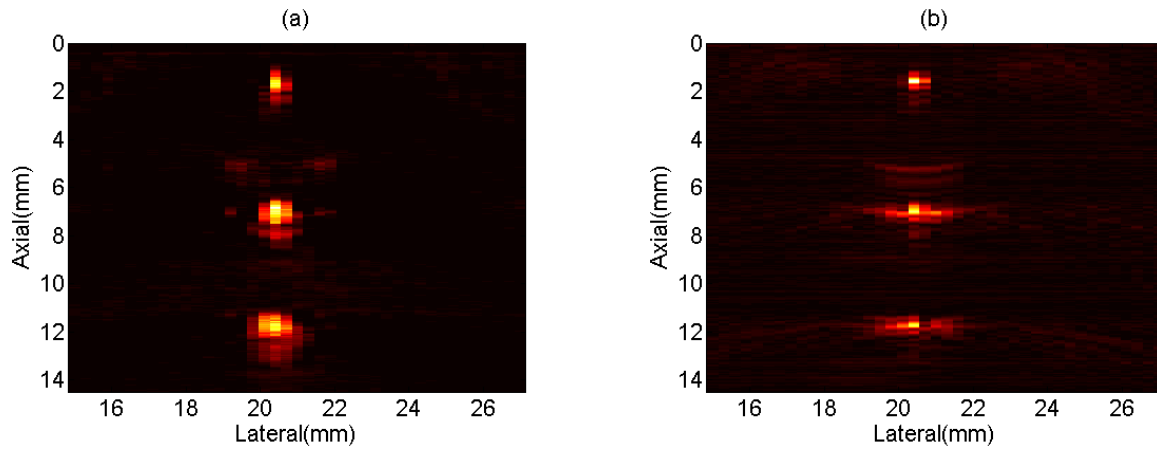
Figure 3: Photoacoustic images of a phantom with three point targets: images reconstructed by (a) short-lag spatial coherence and (b) delay-and-sum beamformed images
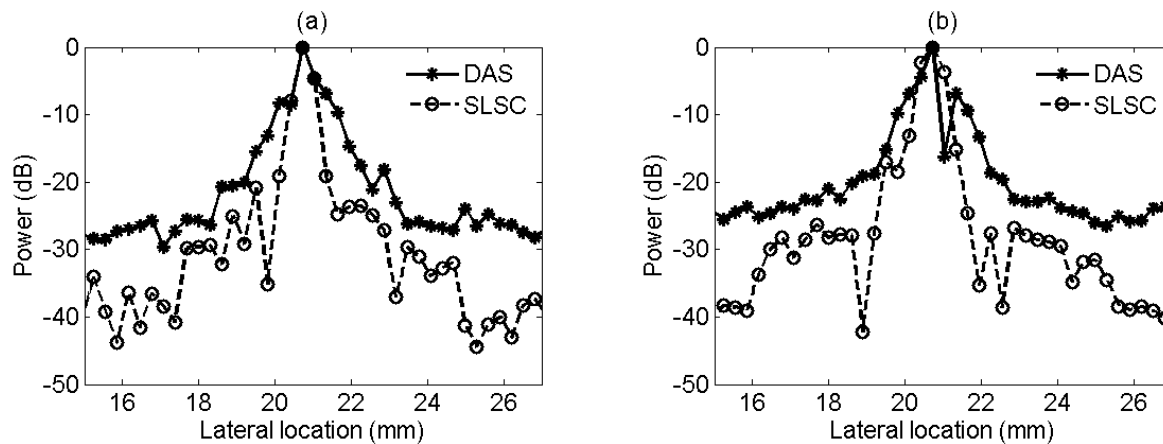

Figure 4: Point spread functions (PSF) at (a) 9 mm and (b) 14 mm away from the surface of the linear array transducer. Circles with dashed lines and asterisks with solid lines indicate PSFs obtained from SLSC and DAS, respectively.

Point spread functions (PSF) at 9 mm and 14 mm away from the surface of the linear array transducer (Figure 1(a)) are presented in Figures 4(a) and 4(b), respectively. The x-axis indicates the lateral locations, which are perpendicular to the imaging plane and parallel to the linear array transducer. The y-axis denotes power in the dB scale. The y-axis values are normalized by the maximum value at the same depth. It is observed that the side lobes, obtained by SLSC are reduced by 5-20 dB when compared to those obtained by DAS. Moreover, the narrower main lobe in Figure 4(a) shows enhanced spatial resolution for the point target at 9 mm, which is closer to the transducer.

To compare the quality of images between techniques, the contrast, contrast-to-noise ratio (CNR), and signal-to-noise ratio (SNR) were measured with an inclusion phantom. The number of data frames needed for optimal image reconstruction was also investigated. SLSC and DAS were applied on each frame of the PA data and then the images were obtained by averaging the results. To compute contrast, CNR, and SNR, two regions of interest (ROIs) were considered inside and outside of the inclusion representing the signal and the background noise. These areas are shown in Figure 5(b) with white rectangles.
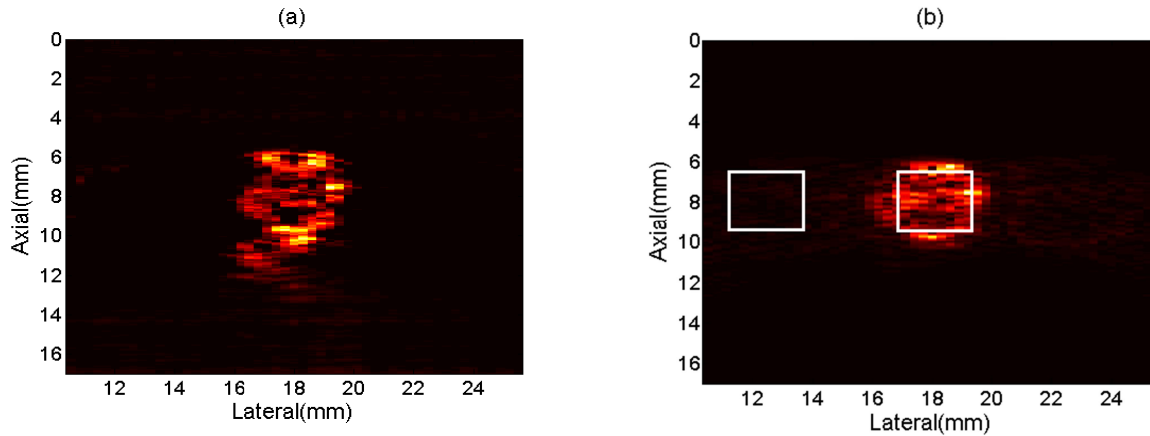
Figure 5: Photoacoustic images of a phantom with an inclusion: images reconstructed by (a) short-lag spatial coherence and (b) delay-and-sum beamforming using 16 frames

Contrast, CNR, and SNR are calculated based to following equations:

$$Contrast = 20log10\left(\frac{S_i}{S_o}\right) \qquad (3)$$

$$CNR = \frac{|S_i - S_0|}{\sigma_0} \qquad (4)$$

$$SNR = \frac{S_i}{\sigma_0} \qquad (5)$$

where S_i and S_o are the mean signals at the same depth inside and outside of the inclusion (signal and noise), σ_o is the standard deviation of the area outside the inclusion (noise). Measurement results are presented in Table 1. For SLSC, the contrast, CNR, and SNR are improved as the number of frames increases. In DAS beamforming, images are reconstructed based on magnitude of the PA signals from optical absorbers. Due to high fluence of each laser pulse in these experiments, the magnitude of PA signals from the inclusion were much stronger than the signals from outside the inclusion. Therefore, images reconstructed with one frame were good enough to provide meaningful information and increasing the number of frames did not influence the results. In SLSC, images are generated by considering spatial coherence which is independent from magnitude of PA signals. Therefore, frame averaging increased the contrast, CNR, and SNR in the SLSC approach.

Table 1 : Contrast, CNR, and SNR in SLSC and DAs for different number of frames

	SLSC 1 Frame	SLSC 8 Frames	SLSC 16 Frames	SLSC 32 Frames	DAS 1 Frame	DAS 8 Frames	DAS 16 Frames	DAS 32 Frames
Contrast (db)	33.8	42.8	44.7	44.9	21.6	21.9	21.7	21.7
CNR	14	31.9	38.2	38.7	21.8	22.4	21.8	21.6
SNR	14.3	32.2	38.4	39	23.8	24.4	23.8	23.5

4. CONCLUSIONS

Clutter can reduce the contrast resolution and detectability of small targets in photoacoustic imaging. In this paper, a short-lag-spatial-coherence (SLSC) imaging technique is implemented to reduce clutter and side lobes and to enhance the main lobe in PA imaging when the ultrasound detection is performed with a linear array transducer. It was assumed that the clutter and side lobes in the PA images have low spatial coherence, and it was shown that SLSC reduces clutter and side lobes and improves image quality.

Two tissue-mimicking phantoms were used to study the performance of SLSC imaging: one which included point targets and another with an extended object (the inclusion). SLSC performance was compared with the conventional delay-and-Sum (DAS) beamforming algorithm. SLSC results showed superior image quality with respect to contrast, contrast-to-noise ratio, and signal-to-noise ratio compared to DAS imaging. The PSF of the point targets also suggested improvement in the spatial resolution and reduction in the side lobes for SLSC beamforming in comparison with DAS beamforming. The image quality was measured by employing a different number of frames when reconstructing the image. The results showed an increase in contrast, CNR, and SNR when SLSC was applied with a greater number of frames. For DAS imaging, the number of frames did not have a significant impact on the results in these experiments.

REFERENCES

[1] Park, S. , Karpiouk, A.B. , Aglyamov, S.R. and Emelianov, S.Y. , "Adaptive beamforming for photoacoustic imaging using linear array transducer," in IEEE Ultrasonics Symposium, IUS 2008, 1088-1091 (2008).

[2] Niederhauser, Joel J., Jaeger, Michael and Frenz, Martin, "Comparision of laser-induced and classical ultasound," Proc. SPIE 4960, Biomedical Optoacoustics IV, 118-123 (2003).

[3] Mallart, Raoul and Fink, Mathias, "The van Cittert-Zernike theorem in pulse echo measurements," Acoustical Society of America, 90(5), 2718-2727 (1991).

[4] Li, M.-L., "Adaptive Photoacoustic imaging using the Mallart-Flink focusing factor," in SPIE International Symposium on Biomedical Optics, San Jose, California, (2008).

[5] Camacho, J., Parrilla, M. and Fritsch, C., "Phase coherence imaging.," IEEE Trans Ultrason Ferroelectr Freq Control, 958-974 (2009).

[6] Mallart, Raoul and Fink, Mathias, "Adaptive focusing in scattering media through sound-speed inhomogeneities: The van Cittert Zernike approach and focusing criterion," The Journal of the Acoustical Society of America, 3721-3732(1994).

[7] Dahl, J.J., Hyun, D., Lediju, M. and Trahey, G.E., "Lesion detectability in diagnostic ultrasound with short-lag spatial coherence imaging.," Ultrason Imaging, 119-133 (2011).

[8] Lediju, M.A., Trahey, G.E., Byram, B.C. and Dahl, J.J., "Short-lag spatial coherence of backscattered echoes: imaging characteristics," IEEE Trans Ultrason Ferroelectr Freq Control, 1377-1388 (2011).

[9] Goodman, J. W., [Statistical Optics] , Wiley Interscience, (2000).

[10] Jakovljevic, M., Dahl, J.J. and Trahey,G.E., "Improved detectability of hypoechoic regions with short-lag spatial coherence imaging: experimental validation," in Proc. SPIE 7968, (2001).